CSTAM2013 - P01 - A0016

The influence of surface roughness characteristics on fatigue stress concentration

J.F. Zhang[1], Q. Li, D. Mu, X.D. Bian

Key Laboratory for Mechanics in Fluid and Solid Coupling Systems, Institute of Mechanics, Chinese Academy of Sciences, Beijing 100190, China, [1]email: zhangjf@imech.ac.cn

Abstract

Numerical simulations have been performed to analyze the influence of surface roughness on the fatigue stress concentration with finite element method (FEM). The parameters to characterize the rough surface topology are analyzed, and the inherent relationships between the characteristic parameters of the rough surfaces are described based on statistical theory. The quantitative mathematical expressions for stress concentrations are given in terms of the dimensionless parameters of rough surface for both plane stress and plane strain states, and the consistent form is summarized. The errors for the stress concentration factor (K_t) and the fatigue stress concentration factor (K_f) predicted from the proposed model were within 4% and 1% of those from FEM numerical simulations. Results show that the standard deviation of the valley radius of the surface profile must be taken into account as an important parameter in the prediction of fatigue stress concentration.

Keywords: fatigue; surface roughness; characteristic parameter; finite element simulation

1. Introduction

Surface roughness is known to affect fatigue life of structural components seriously, and it is usually characterized through the height distribution (z) of recorded geometric profile, in respect to the mean line over the assessment length L, such as R_a (average roughness), R_y (peak-to-valley height roughness) or R_z (10-point roughness) [1, 2].

Researchers took the effect of surface roughness on the fatigue strength of structures as integrative stress concentration effect of microscope notch. This stress concentration effect can be described through the fatigue stress concentration factor K_f which is related to the stress concentration factor K_t [3].

$$K_f = 1 + q(K_t - 1) \tag{1}$$

where q is the notch sensitivity, depending on the material and asperities geometry. It can be defined in terms of the effective profile valley radius of the surface texture [4].

$$q = \frac{1}{1 + \gamma/\rho} \tag{2}$$

in which γ is a material constant.

Neuber also proposed an expression for estimating the stress concentration factor.

$$K_t = 1 + n\sqrt{\xi \frac{R_z}{\rho}} \tag{3}$$

where n represents the stress state (n=1 for shear and n=2 for tension), ρ the effective profile valley radius of the surface texture, and ξ the ratio between spacing and depth of the asperities.

Arola *et al* proposed a different stress concentration factor expression for the process-dependent surface texture [5, 6].

$$K_t = 1 + n\left(\frac{R_a}{\overline{\rho}}\right)\cdot\left(\frac{R_y}{R_z}\right) \tag{4}$$

where $\overline{\rho}$ is the average radius determined from the dominant profile valleys.

Andrews and Sehitoglu also used geometric parameters to produce a logical surface for calculation of stress concentration factors and performed fatigue prediction based on the fracture mechanics approach accounting for crack closure effect [7].

However, the standard roughness parameters constitutes a simple way of quantifying profile height distributions, it is not able to provide all specific features of the surface that are important to fatigue life [1,2,6]. The result is that it washes out information on potentially critical surface grooves [8].

Recently, the stress concentration factor K_t is found by finite element analysis of the measured surface topography rather than the averaged geometrical parameters, which is more representative of what the samples really undergo. It is expected to yield more accurate fatigue life prediction by characterizing a surface topography [1].

In the present paper, the parameters characterizing surface roughness are analyzed, and the relationships between the characteristic parameters are deduced based on statistical theory. A time series approach is adopted to generate logical random surface, and the relationships between stress concentration factor and those dimensionless influencing parameters are obtained in terms of FEM numerical simulation. Comparison of calculating results from several models is also carried out.

2. Characterization of Rough Surface

Surface roughness is taken as spatial geometric characterization of surface profile. From the viewpoint of mathematics, for a deterministic problem, the number of independent parameters should be equal to the number of independent coordinates. Now the surface topography is taken as a stochastic process, for each spatial direction, it must be described by two statistical variants, namely, the mean and the deviation. For convenience, 2D surface is chosen in the following discussion.

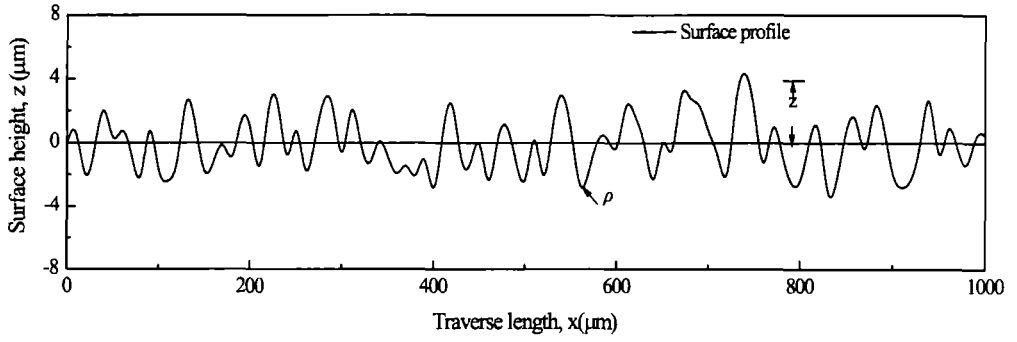

Fig. 1. Surface profile and definitions of parameters

An example of 2D surface profile is shown in Fig.1, it may be expressed as

$$z = h \cdot \sin \omega x \tag{5}$$

where h and ω are independent random variations, representing the amplitude of surface height z and the circular frequency relating to the characteristic wavelength λ, respectively, and $\omega = 2\pi/\lambda$.

At each tip of the surface valley, the derivative z' should be zero, *i.e.* $\cos\omega x_i = 0$, and $\sin\omega x_i = 1$. The tip radius can be given below.

$$\rho = \left|\frac{(1+z'^2)^{3/2}}{z''}\right| = \left|\frac{1}{z''}\right| = \frac{1}{\omega^2 h} = \frac{\lambda^2}{4\pi^2 h} \tag{6}$$

It is apparent that the tip radius ρ of surface valley is dependent on the local parameters h and ω. Hence, for a 2D stochastic surface roughness, there are four parameters to describe its geometric characteristics, i.e. the means ($\bar{h}$ and $\bar{\rho}$) and the standard deviations (h_{sd} and ρ_{sd}).

Based on statistical theory, the traditional roughness parameters, such as R_a, R_y, and R_z, can be determined in terms of the mean and standard deviation of the independent variant h under a certain probability distribution and reliability. For instance, one can easily give the expression of R_a as

$$R_a = \frac{1}{L}\int_0^L z(x)dxdx = \frac{1}{L}\int_0^L \int_0^{+\infty} \int_{-\infty}^{+\infty} h\cdot\left|\sin\omega x\right|\cdot f(h,\omega)d\omega dhdx = \frac{2}{\pi}\bar{h} \tag{7}$$

in which $f(h,\omega)$ denotes the joint probability density function of the surface amplitude h and local circular frequency ω.

Assuming the surface amplitude to be subjected to log-normal distribution with a log domain mean $\bar{h}^*$ and a log domain standard derivation h_{sd}^*, the probability density function of the surface amplitude h is expressed in Eq. 8, and the relationships between the parameters $\bar{h}$, h_{sd}, $\bar{h}^*$, and h_{sd}^* are given in Eq. 9 and Eq. 10.

$$f(h) = \frac{1}{h\cdot h_{sd}^*\cdot\sqrt{2\pi}}\exp\left[-\frac{1}{2}\left(\frac{\ln h-\bar{h}^*}{h_{sd}^*}\right)^2\right] \tag{8}$$

$$\bar{h} = \exp\left(\bar{h}^* + \frac{1}{2}h_{sd}^{*\,2}\right) \tag{9}$$

$$h_{sd} = \left[\exp\left(h_{sd}^{*\,2}\right)-1\right]\cdot\exp\left(2\bar{h}^* + h_{sd}^{*\,2}\right) \tag{10}$$

Then, R_y can be obtained by the following expression.

$$R_y = 2\cdot\exp\left(\bar{h}^* + mh_{sd}^*\right) \tag{11}$$

where m is a constant determined by the probability distribution of h_{sd}^* and a certain reliability.

In practice, it is difficult to measure the wavelength λ for a random surface topography. The alternative parameters R_a and ρ (tip radius of valley) may be better for both understanding and measurement. Thus, the dimensionless parameters characterized the spatial geometry of surface topography should be reselected as $R_a/\bar{\rho}$, R_y/R_a, and $\rho_{sd}/\bar{\rho}$. The relationships between R_a, $\bar{\rho}$, R_y, $\bar{h}$ and $\bar{\lambda}$ are given by Eq. 6, Eq. 7 and Eq. 11, respectively.

3. Numerical Generation of Rough Surface Profiles

The surface amplitude h and the tip radius of surface valley ρ are still taken as statistical variations. They are all assumed to be subjected to log-normal distributions. According to Eq.5 and Eq.6, the surface profile can be generated by the following formula.

$$z = h \cdot \sin\frac{2\pi}{\lambda}x = h \cdot \sin\frac{1}{\sqrt{\rho h}}x \tag{12}$$

To construct the surface profile, Excel Spreadsheet is adopted. Under the specific characteristic parameters, a control number is set to ensure a complete period be generated for each combination of random parameters h and ρ. To avoid singularity and ensure the precision of FEM simulation, at least 30 points are generated for each period with respect to the characteristic wavelength.

Examples of surface profiles with log-normal distributions for the tip radius of the surface valleys and the amplitude of the surface height are shown in Fig. 2.

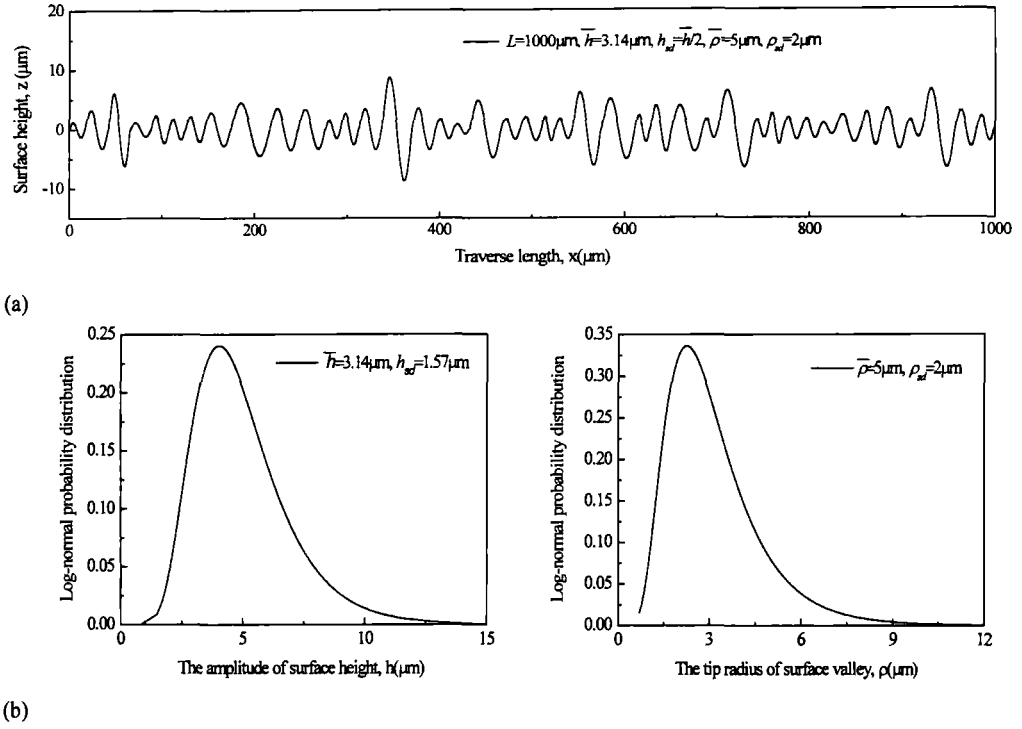

Fig. 2. Examples of surface profiles with different means and standard deviations: (a) for Case I; (b) the log-normal distribution of the characteristic parameters

4. Numerical Simulations

The constructed surface profile is used to generate FEM geometry. The size of the elements adjacent to the rough surface in the FEM model is about 1/30 of the characteristic wavelength. An example of such a 2D model with FEM mesh is shown in Fig.3. Material behavior is linear elastic with Young's modulus E=2.0×10^{11} Pa and Poisson's ratio ν=0.29. To ensure precision, a higher order 8-node element with quadratic displacement behavior is used for meshing. It provides more accurate results for mixed (quadrilateral-triangular) meshes and can tolerate irregular shapes without as much loss of accuracy. The contours of Von Mises stresses are also shown in Fig. 3.

According to the above analysis, the dimensionless characteristic parameters are R_a /, R_y /R_a, and $\rho_{sd}/\bar{\rho}$. To probe the influences of the three dimensionless parameters on stress concentration by FEM numerical simulation, eight cases are adopted for each dimensionless parameter and ten surface profile samples are generated for each case. The average values of the stress concentration factors are calculated for both plane stress and plane strain states, as shown in Fig. 4, and the expressions for the stress concentration factors are obtained by data fitting.

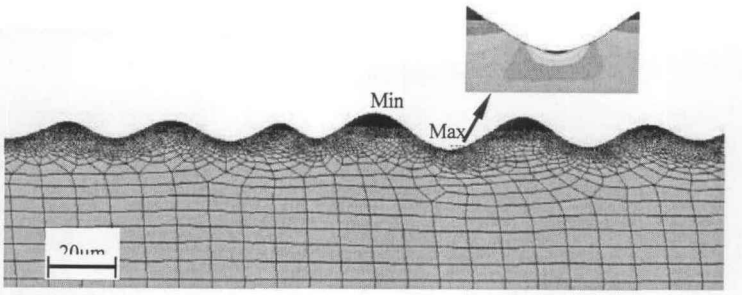

Fig. 3. FEM model and the distribution of stress

$$K_t = 1 + 1.017\left(\frac{R_a}{\bar{\rho}}\right)^{0.375}\left(\frac{R_y}{R_a}\right)^{0.474}\left[2.24 - \frac{1.24}{1+2.45\left(\rho_{sd}/\bar{\rho}\right)^{1.88}}\right] \quad \text{(for plane stress state)} \tag{13}$$

$$K_t = 1 + 0.791\times\left(\frac{R_a}{\bar{\rho}}\right)^{0.388}\left(\frac{R_y}{R_a}\right)^{0.51}\left[2.72 - \frac{1.72}{1+2.42\left(\rho_{sd}/\bar{\rho}\right)^{1.97}}\right] \quad \text{(for plane strain state)} \tag{14}$$

Combining Eq. 13 and Eq. 14, the consistent form of the stress concentration factor for 2D surface profile can be rewritten as

$$K_t = 1 + A\left(\frac{R_a}{\bar{\rho}}\right)^{0.4}\left(\frac{R_y}{R_a}\right)^{0.5}\left(2 - \frac{1}{1+2\left(\rho_{sd}/\bar{\rho}\right)^2}\right) \tag{15}$$

in which the coefficient A=1 and 0.8 for plane stress and plane strain states respectively.

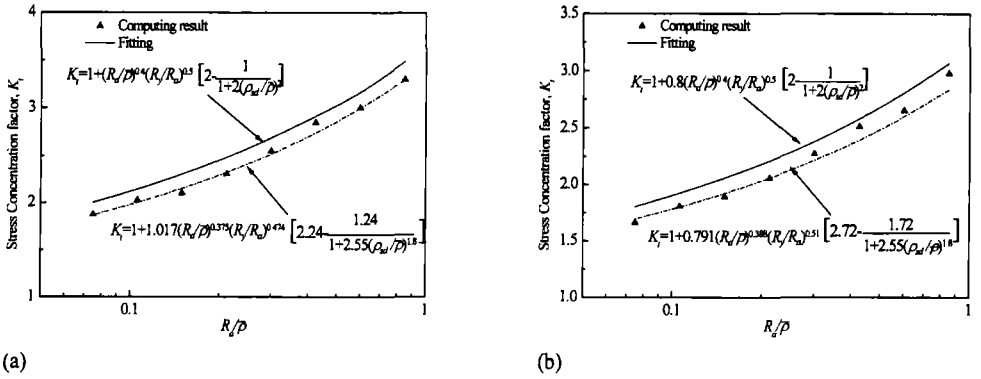

Fig. 4. Stress concentration factor K_t versus Ry/Ra: (a) for plane stress; (b) for plane strain

To verify the precision of Eq. 15, FEM simulations are also conducted, and the results are illustrated in Fig. 4. It is shown that the predicted results are consistent with FEM results. The maximum error is 4.1%.

Results from Eq. 15, the Neuber rule, and the Arola–Ramulu model, as well as from FEM simulations are compared for the AWJ machined surfaces in literature [6]. The predicted results of stress concentration K_t are shown in terms of the surface roughness R_a in Fig. 5(a). The fatigue stress concentration K_f obtained by Eq. 15, Eq. 1 and Eq. 2 are illustrated in Fig. 5(b).

It is apparent from Fig. 5(b) that predictions for K_f obtained from Eq. 15 are more consistent with that obtained by FEM simulation. The maximum errors for the stress concentration factors (K_t) and the fatigue stress concentration factors (K_f) are 3.3% and 0.61%, respectively. In fact, the standard deviations ρ_{sd} make the effective profile valley radius of the surface texture sharper than the average valley radius. Hence, the standard deviation of the profile valley radius of the surface texture must be taken into account as an important parameter influencing stress concentration.

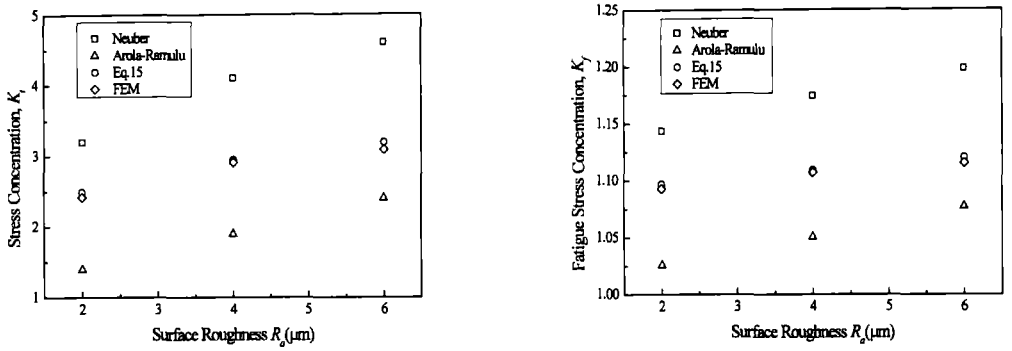

(a) (b)

Fig. 5. Stress concentration of the AWJ machined surface: (a) stress concentration factors K_t; (b) fatigue stress concentration factors K_f

5. Conclusion

Based on analysis of the characteristic parameters of surface roughness and the results from FEM simulation, the following conclusions can be drawn.

1) The spatial geometry of random surface topography can be characterized by the dimensionless parameters $R_a/\overline{\rho}$, R_y/R_a, and $\rho_{sd}/\overline{\rho}$.
2) Average surface roughness can't sufficiently interpret the fatigue stress concentration since it does not account for the process-dependent profile valley radii. As indicated in Section 1, the standard deviation of the profile valley radius of the surface profile must be taken into account as an important influencing parameter in the prediction of fatigue stress concentration.
3) The stress concentration factor (K_t) for rough surfaces can be evaluated with Eq. 15. Comparing with the Neuber rule and Arola–Ramulu model, results from Eq. 15 are more consistent with that from FEM numerical simulations

Acknowledgements

This work was financially supported by the National Key Foundation Research Program (6150804).

References

[1] Suraratchai M, Limido J, Mabru C, Chieragatti R. Modelling the influence of machined surface roughness on the fatigue life of aluminium alloy. *Int J Fatigue* 2008; **30**: 2119–26.

[2] Ås SK, Skallerud B, Tveiten BW, Holme B. Fatigue life prediction of machined components using finite element analysis of surface topography. *Int J Fatigue* 2005; **27**: 1590–6.

[3] Peterson RE. *Stress concentration factors*. New York: John Wiley and Sons; 1974.

[4] Neuber H. *Kerbspannungslehre*. Berlin, Germany, Springer-Verlag;1958.

[5] Arola D, Ramulu M. An examination of the effects from surface texture on the strength of fiber-reinforced plastics. *J Compos Mater* 1999; **33**: 101–86.

[6] Arola D, Williams CL. Estimating the fatigue stress concentration factor of machined surfaces. *Int J Fatigue* 2002; **24**: 923–30.

[7] Andrews S, Sehitoglu H. A computer model for fatigue crack growth from rough surfaces. *Int J Fatigue* 2000; **22**: 619–30.

[8] Ås SK, Skallerud B, Tveiten BW. Surface roughness characterization for fatigue life predictions using finite element analysis. *Int J Fatigue* 2008; **30**: 2200–9.